RESEARCH PAPER

Theoretical study of small clusters of manganese-doped gallium oxide: $Mn(GaO)_n$ and $Mn_2(GaO)_n$ with $n = 1-7$

Amol Rahane · Mrinalini Deshpande ·
Ravindra Pandey

Abstract Structures, electronic and magnetic properties of Mn and Mn_2 doped stoichiometric $(GaO)_n$ clusters with $n = 1-7$ are studied in the framework of density functional theory. Doping of a Mn atom is found to be energetically favorable in $(GaO)_n$ clusters and the equilibrium configurations are found to be determined by the metal–oxygen interactions. Mn prefers to maximize the number of Mn–O bonds by selecting a Ga site in the cluster which increases its coordination with oxygen. Addition of a Mn atom in $Mn(GaO)_n$ clusters results into the ground state to be either ferromagnetic or antiferromagnetic depending on the Mn coordination number and the Mn–Mn bond-length in the given $Mn_2(GaO)_n$ cluster.

Keywords DMS materials · Mn-doped gallium oxide clusters · Magnetic properties · Density functional theory · Semiconductors · Modeling and simulation

A. Rahane · M. Deshpande (✉)
Department of Physics, H.P.T. Arts and R.Y.K Science
College, Nasik, Maharashtra, India
e-mail: mdd@mtu.edu

M. Deshpande · R. Pandey
Department of Physics, Michigan Technological
University, Houghton, MI 49931, USA

Introduction

Dilute magnetic semiconductors have been a focus of several experimental and theoretical studies due to their potential applications in spin-dependent electronic devices. They are formed by the partial substitution of the cations with a small amount of magnetic transition metal ions in the crystalline lattice. In the conventional dilute magnetic semiconductors, such as $Ga_{1-x}Mn_xAs$ ferromagnetism exists far below the room temperature restricting their applications in electronic devices. In recent years, the wide gap semiconductors such as ZnO, GaN, and Ga_2O_3 doped with manganese are found to have high Curie temperature (Dietl et al. 2000; Song et al. 2006). Specifically, experimental studies on $Ga_{(2-2x)}Mn_{2x}O_3$ $(x = 0.05, 0.10)$ polycrystalline material have found a direct relationship between the dopant concentration and the magnetization effects (Lee et al. 2004). It was then suggested that a detailed analysis of local environment of Mn is necessary to understand the increase in the magnetization effect with Mn concentration in the oxide lattice.

The microstructure of thin films of Mn-doped Ga_2O_3 was explored in detail using the spectroscopic techniques. It was concluded that the divalent Mn ions are located at the tetrahedral site in the oxide lattice (Huang et al. 2007). This is consistent with the results of the atomistic simulation study where small doubly charged dopants are predicted to prefer the

tetrahedral coordination in the lattice. On the other hand, the trivalent dopants are predicted to be stabilized at the octahedral gallium sites in Ga_2O_3 (Blanco et al. 2005; Hayashi et al. 2006). A recent first principles study for Mn-doped β-Ga_2O_3 has, however, found that when a Ga ion replaced with a single Mn ion, the octahedral site becomes more stable as compared to the tetrahedral site in the cation sublattice. Furthermore, a ferromagnetic coupling between Mn atoms occurs when they substitute either tetrahedral or octahedral coordinated Ga sites. On the other hand, the antiferromagnetic interaction stabilizes the oxide lattice when Mn atoms substitute Ga having different coordination in the lattice (Pei et al. 2008).

In the present study, our aim is now to understand the coordination-dependent ferromagnetism in Mn-doped β-Ga_2O_3 at nanoscale for which we consider small clusters of Mn and Mn_2-doped $(GaO)_n$. Electronic structure calculations on the doped $(GaO)_n$ clusters will reveal that the preferential substitutional site for Mn is the site with a maximum coordination number. In the case of Mn_2-doped $(GaO)_n$, the predicted stability of ferromagnetic and antiferromagnetic states is found to be sensitive to the Mn coordination number and the Mn–Mn bond length.

Rest of the paper is organized as follows: Second section describes our computational methodology. The results are presented and discussed in third section, and summarized the results in fourth section.

Fig. 1 Schematic representation of some of the initial configurations considered for Mn(GaO)$_n$, ($n = 1-7$) clusters. The *hollow spheres* represent the Ga-atoms, the *dark spheres* represent the O-atoms and solid sphere represents the Mn-atom
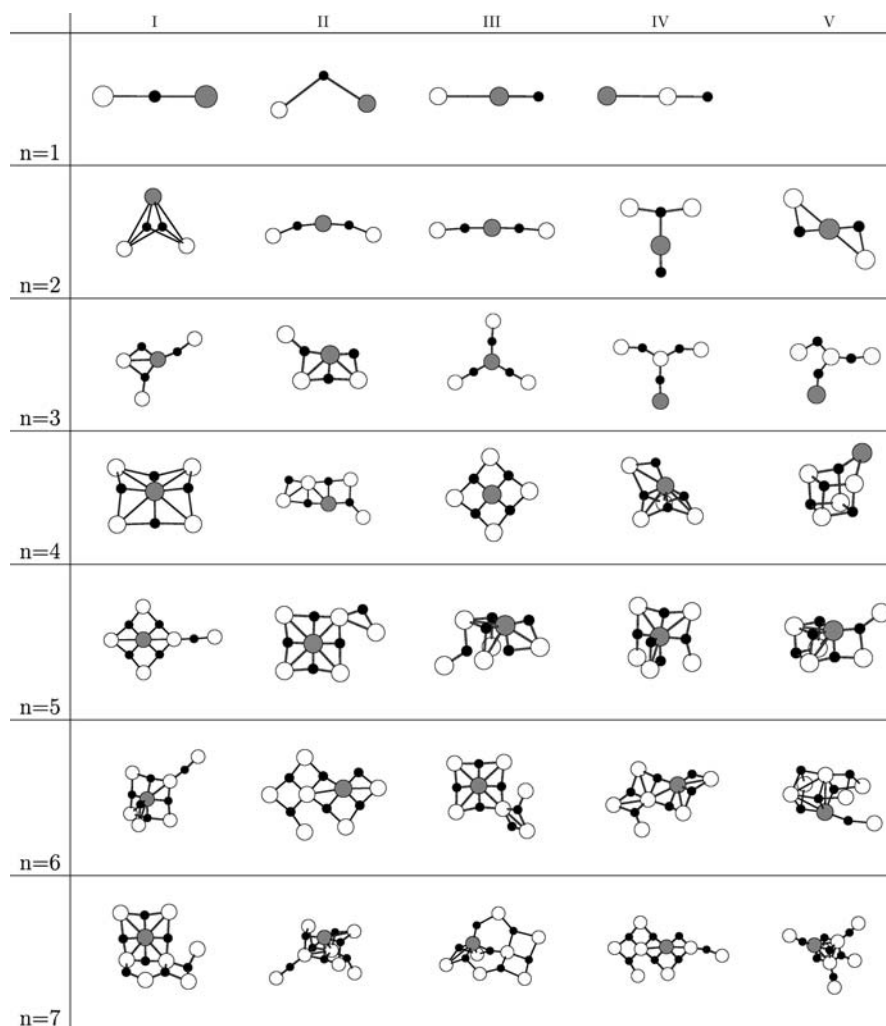
Computational details

First principles calculations were performed using the spin polarized density functional theory within the generalized gradient approximation (GGA) given by Perdew–Bruke–Ernzerhof (Perdew et al. 1996). The projector augmented wave (PAW) method (Blöchl 1994; Kresse and Joubert 1999) as implemented in the Vienna ab initio Simulation Package (Kresse and Furthmuller 1996; VASP 1999) was used.

The clusters considered were placed in a cubic supercell with an edge of 20 Å and periodic boundary conditions were imposed. The cutoff energy for the plane wave was set to 282.8 eV. The calculations were considered to be converged when the force on each ion was less than 0.001 eV/Å with a convergence in the total energy of about 10^{-5} eV.

The equilibrium geometries of the clusters were obtained by quenching a large number of planar and nonplanar configurations of $Mn(GaO)_n$ and $Mn_2(GaO)_n$ clusters using the quasi-Newton method (VASP 1999). The choice of some of the initial geometries was partially dependent upon our previous studies of small clusters of gallium oxide (Gowtham et al. 2004; Gowtham et al. 2005; Deshpande et al. 2006). While doping of Mn atom in the pure gallium oxide clusters we have considered all the possible sites for Mn atom in the cluster. The stability of the cluster is further verified by performing the calculations with singlet (doublet) or higher spin states depending on an even (odd) number of valence electrons in the system.

Fig. 2 Schematic representation of some of the initial configurations considered for $Mn_2(GaO)_n$, ($n = 1-7$) clusters. The *hollow spheres* represent the Ga-atoms, the *dark spheres* represent the O-atoms and *solid spheres* represent the Mn-atoms
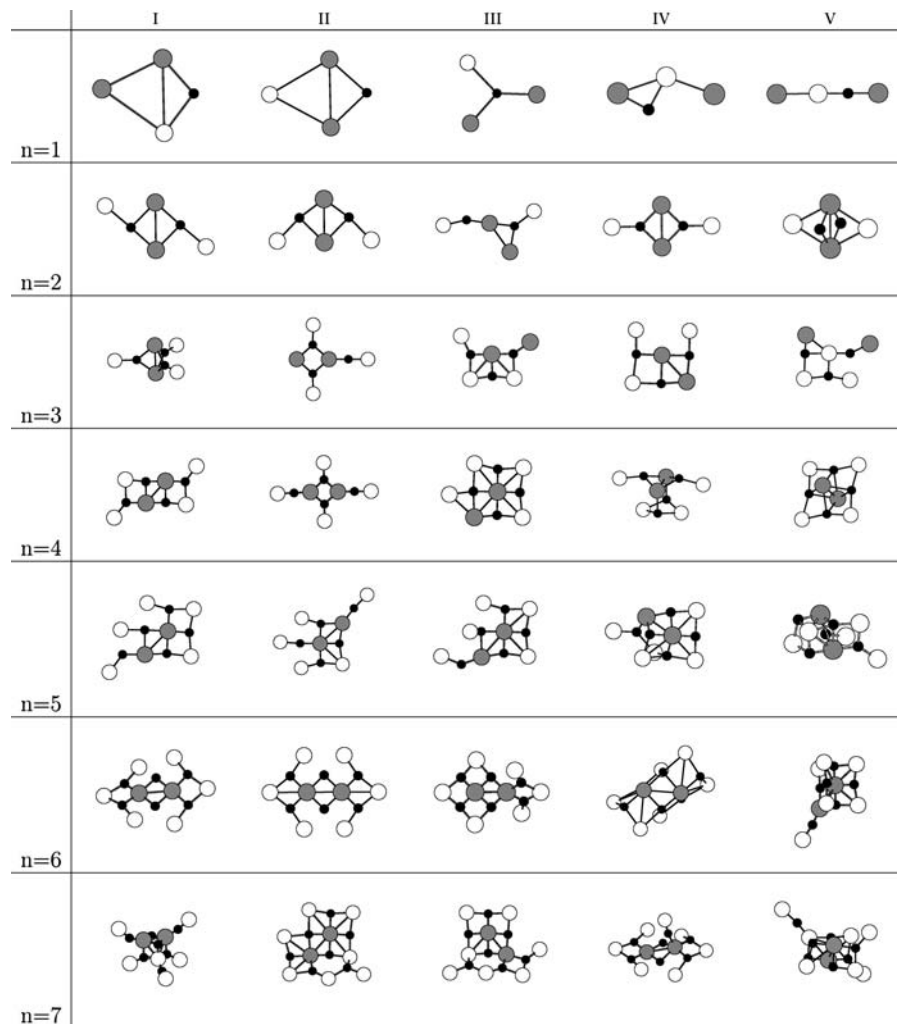
Results and discussion

Some of the initial configurations of $Mn(GaO)_n$ and $Mn_2(GaO)_n$, $(n = 1-7)$ clusters considered are schematically represented in Figs. 1 and 2, respectively. The lowest-energy configurations, referred to as the
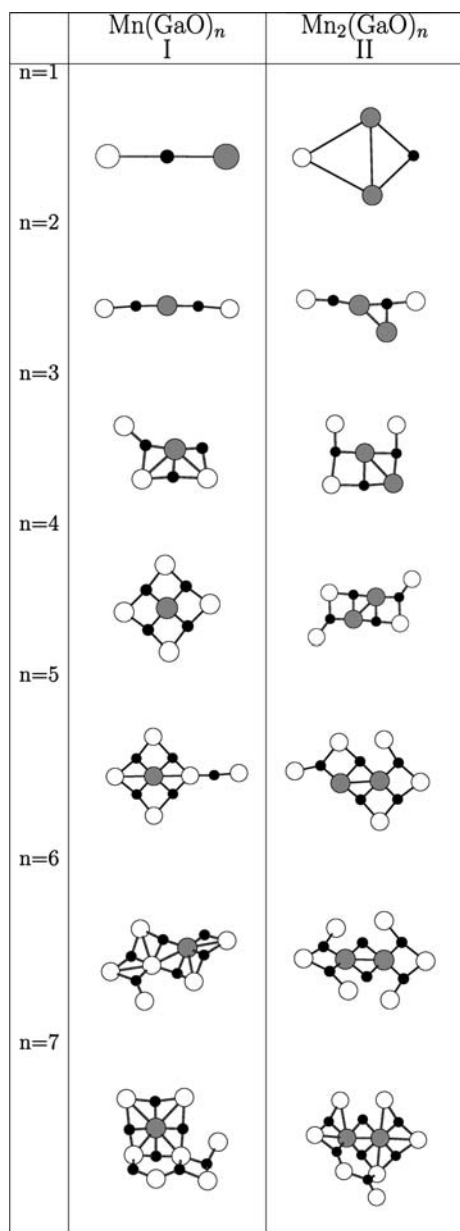
Fig. 3 The ground state configurations of $Mn(GaO)_n$, and $Mn_2(GaO)_n$, $(n = 1-7)$ clusters. The *hollow spheres* represent the Ga-atoms, the *dark spheres* represent the O-atoms and *solid spheres* represent the Mn-atoms

ground state configurations, of these clusters are shown in Fig. 3-I, II. In Tables 1 and 2, we present total energy, magnetic moment, binding energy, and interatomic distances corresponding to the ground state configurations of the oxide clusters.

$Mn(GaO)_n$ Clusters, $(n = 1-7)$

The ground state of $Mn(GaO)$ is predicted to be a oxygen centered linear chain of Ga–O–Mn (Fig. 3-I) with GaO and MnO bond distances (R_{Ga-O} and R_{Mn-O}) are 3.52 and 1.82 Å, respectively. The bent configuration (Fig. 1-II) is nearly degenerate with the linear one $\Delta E \approx 0.03$ eV. The ground state of $Mn(GaO)_2$ can be considered as a OMnO molecule terminated by two Ga atoms. Here, R_{Ga-O} and R_{Mn-O} are 1.83 and 1.81 Å, respectively. A preference for the metal-oxygen bond over the metal-metal bond is predicted in $Mn(GaO)_2$ as one would expect from the trend in the computed binding energies of MnO, GaO, and GaMn molecules. The calculated binding energy of MnO is 2.86 eV/atom which is higher than that of GaO (2.45 eV/atom). On the other hand, GaMn and Mn_2 are weakly bonded systems with the binding energies of 0.75 and 0.54 eV/atom and the bond length of 2.57 and 2.58 Å, respectively.

Addition of a GaO molecule to $Mn(GaO)_2$ results into a 2D window-pane configuration where Mn prefers to sit on the site which can maximize the number of Mn–O bonds in the cluster. The other low-lying isomers consisting of the rhombus and Y-shaped configurations (Fig. 1-I, III) are well above the ground state with $\Delta E = 0.26$ and 0.55 eV, respectively. Note that the ground state configuration maximizes the overall Mn–O and Ga–O interactions in the cluster as compared to the other low-lying configurations.

The ground state configuration of $Mn(GaO)_4$ is a Mn-centered square configuration where each side consists of a Ga–O–Ga chain. Here, R_{Mn-O} is 1.86 Å and R_{Ga-O} is 2.02 Å. The equilibrium configuration of $Mn(GaO)_5$ is predicted to be a kite configuration in which the additional (GaO) molecule gets attached to one of the Ga atom. By preferring quasiplanar configuration, $Mn(GaO)_6$ follows the same trend as that of $Mn(GaO)_5$. With MnO_4 unit, the addition of GaO maximizes the number of Ga–O bonds in the cluster. The ground state configuration of $Mn(GaO)_7$ is a three-dimensional (3D) configuration.

Table 1 Total energy (eV), magnetic moment (μB), binding energy (eV/atom), HOMO–LUMO (HL) gap (eV), and bond lengths (Å) of the ground state configurations of Mn(GaO)$_n$, ($n = 1-7$) clusters

System	Total eng. (eV)	μB	BE (eV/atom)	HL gap (eV)	R_{Ga-O} (Å)	R_{Mn-O} (Å)
(GaO)	−497.88	1	2.45	4.63	1.73	–
Mn(GaO)	−923.76	6	2.94	2.30	1.84	1.83
(GaO)$_2$	−999.5635	0	3.41	3.18	1.76	–
Mn(GaO)$_2$	−1426.3264	5	3.68	3.42	1.83	1.81
(GaO)$_3$	−1500.8537	1	3.66	3.04	1.93	–
Mn(GaO)$_3$	−1927.7306	4	3.83	1.01	2.02	1.82
(GaO)$_4$	−2002.7781	0	3.87	3.64	1.83	–
Mn(GaO)$_4$	−2429.4526	3	3.95	0.56	2.02	1.86
(GaO)$_5$	−2503.6262	1	3.88	3.12	1.78	–
Mn(GaO)$_5$	−2930.7817	4	4.00	2.03	1.78	1.84
(GaO)$_6$	−3005.6181	0	3.98	3.41	1.79	–
Mn(GaO)$_6$	−3431.6554	3	4.00	0.49	1.88	1.71
(GaO)$_7$	−3506.6412	1	3.99	2.36	1.78	–
Mn(GaO)$_7$	−3933.3241	4	4.04	1.78	1.76	1.83

Table 2 State, total energy (eV), magnetic moment (μB), binding energy (eV/atom), HOMO–LUMO gap (eV), and bond lengths (Å) of the ground state configurations of the Mn$_2$(GaO)$_n$, ($n = 0-7$) clusters

System	State	Total eng. (eV)	ΔE (eV)	μB	BE (eV/atom)	HL gap (eV)	R_{Ga-O} (Å)	R_{Mn-O} (Å)	R_{Ga-Mn} (Å)	R_{Mn-Mn} (Å)
Mn$_2$	FM	−845.02		10	0.54	–	–	–	–	2.58
Mn$_2$(GaO)	FM	−1347.08	0.0	9	2.54	1.0317	3.52	1.82	2.52	2.47
	AFM		0.28	1						2.98
Mn$_2$(GaO)$_2$	AFM	−1849.6629	0.0	0	3.29	0.9549	1.84	1.79	2.87	2.60
	FM		0.03	10						2.70
Mn$_2$(GaO)$_3$	FM	−2351.6316	0.0	9	3.61	0.9502	2.01	1.92	2.88	2.63
	AFM		0.1	1						2.44
Mn$_2$(GaO)$_4$	AFM	−2854.4097	0.0	0	3.87	1.4732	1.87	1.87	2.96	2.61
	FM		0.2	10						2.81
Mn$_2$(GaO)$_5$	FM	−3356.3916	0.0	9	3.97	1.8757	1.88	1.86	2.90	2.80
	AFM		0.79	1						2.56
Mn$_2$(GaO)$_6$	AFM	−3858.5291	0.0	0	4.05	1.4522	1.97	1.85	2.93	2.71
	FM		0.08	8						2.76
Mn$_2$(GaO)$_7$	AFM	−4359.0179	0.0	1	4.02	1.3052	1.92	1.86	2.79	2.63
	FM		0.19	7						2.77

FM refers to ferromagnetic and AFM refers to anti-ferromagnetic state of the cluster

For larger clusters with $n > 3$, it is observed that the Mn centered square configuration serves as a building block and structures are stabilized when the coordination of Mn is four. A typical molecular isodensity surface of one of the molecular orbitals of Mn(GaO)$_4$ is shown in Fig. 4. There is a strong localized charge density distribution between Mn to oxygens; Mn$_{d_{x2-y2}}$ hybridizing with O$_p$'s in the cluster. It is interesting to compare the ground state configurations of Mn(GaO)$_4$ and Ga$_4$(MnO$_4$). MnO$_4$ is a distorted tetrahedron configuration with C$_{2v}$ symmetry (Gutsev et al. 1999). Addition of four Ga atoms to MnO$_4$ forces all the oxygen atoms to be coplanar with the Mn atom. Each Ga atom binds with two oxygen atoms with a large apex angle which tends to facilitate a stronger coupling between Ga$_s$ and O$_p$ orbitals in the cluster (Deshpande et al. 2006)
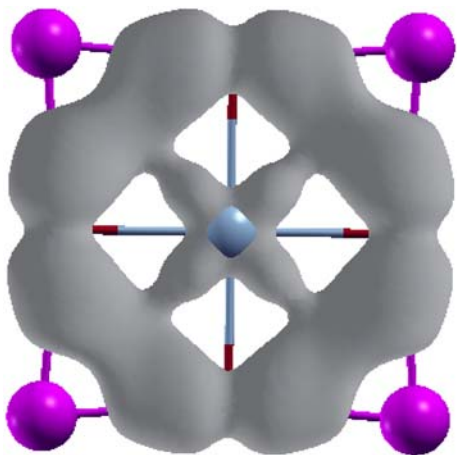
Fig. 4 (Color online) Isodensity surface corresponding to the (HOMO-18) state of Mn(GaO)$_4$, at one-fifth of its maximum isosurface value

The calculated binding energy[1] of the clusters is given in Table 1. Mn tends to stabilize the host oxide cluster indicating that the addition of a single Mn atom is energetically preferred. The charge density isosurfaces (not shown) suggest the bonding between Ga–O is ionic and Mn–O is partly ionic. It is also noted via the charge density contours that the bonding characteristics remain the same in the series.

We now turn our attention to the magnetic properties of the Mn(GaO)$_n$ clusters. The values of the magnetic moments of Mn(GaO)$_n$ lie in the range of 3–6 μB showing a large increase in the magnetic moment of the host oxide cluster due to addition of a Mn atom. Recall that the electronic configuration of a Mn atom is $3d^5 4s^2$ and the magnetic moment of free Mn, Ga, and O atoms are 5, 1, and 2 μB, respectively. In MnO, Mn-4s^2 electrons mainly interact with O-2p electrons whereas Mn-3d^5 electrons do not take part in the bonding yielding the magnetic moment of MnO to be 5 μB. In Mn(GaO), the ionic character of MnGaO cluster leads to the net magnetic moment of 6 μB. As we increase the size of the cluster, the increase in coordination of Mn increases the degree of hybridization between Mn$_d$ and O$_p$ orbitals. The magnetic moment, therefore, decreases to 3 μB in

---

[1] The binding energy per atom (E_b) is defined as

$$E_b[(GaO)_n Mn_m] = (-E[(GaO)_n Mn_m] + n(E[Ga] + E[O]) + mE[Mn])/(2n + m),$$

where E is the total energy of the system.

Mn(GaO)$_4$. For larger clusters, the magnetic moment oscillates between 3 and 4 μB with even or odd number of electrons.

Mn$_2$(GaO)$_n$ Clusters, ($n = 1-7$)

Figure 2 shows some of the structures considered for Mn$_2$ doped gallium oxide clusters. Figure 3-II presents the ground state configurations of Mn$_2$(GaO)$_n$ clusters with $n = 1-7$. Table 2 collects total energy, magnetic moment, binding energy, and interatomic distances of the ground state configurations of these clusters.

The calculated ground state of Mn$_2$(GaO) is a planar (distorted) rhombus structure with R$_{Mn-O}$ = 1.82 Å, and R$_{Ga-O}$ = 3.52 Å. R$_{Mn-Mn}$ is 2.47 Å which is slightly smaller than that in Mn$_2$. The two isomeric configurations (Fig. 2-II, III) are 0.35 and 0.38 eV, respectively higher in energy than the ground state. The ground state configuration of Mn$_2$(GaO)$_2$ is a chain-like atomic arrangement with R$_{Mn-Mn}$ of 2.60 Å. The magnetic moment of this configuration is 0 μB. The ferromagnetic (FM) chain-like configuration is nearly degenerate $\Delta E = 0.03$ eV where the Mn–Mn distance increases by 3% relative to that of the antiferromagnetic (AFM) configuration. The ground state of Mn$_2$(GaO)$_3$ is the window-pane configuration with two terminal Ga atoms. It is similar to the ground state of Mn(GaO)$_3$. Here, R$_{Mn-Mn}$ is 2.63 Å. The rhombus-like configuration (Fig. 2II) is slightly higher in energy $\Delta E \approx 0.16$ eV. The ground state of Mn$_2$(GaO)$_4$ is the extended window-pane configuration where both Mn atoms are linked to three oxygen atoms. The second Mn added to Mn(GaO)$_5$ substitutes the Ga atom having
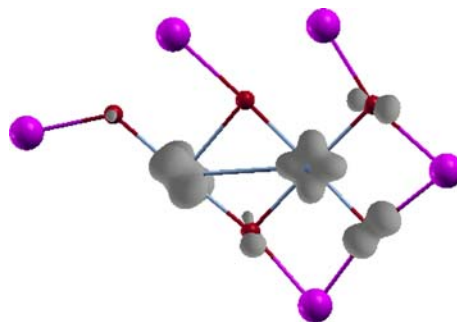
Fig. 5 (Color online) The contour plot of the HOMO of the ground state configuration of Mn$_2$(GaO)$_5$, at one-sixth of its maximum isosurface value

Fig. 6 (Color online) Total spin density $[\rho_\uparrow(\mathbf{r}) - \rho_\downarrow(\mathbf{r})]$ isosurface of $Mn_2(GaO)_6$—AFM and FM configurations, at one-sixth of its maximum isosurface value. *Red* and *blue* surfaces represent positive and negative spin densities, respectively

$Mn_2(GaO)_6$
AFM Configuration (0 μB)

FM Configuration (8 μB)
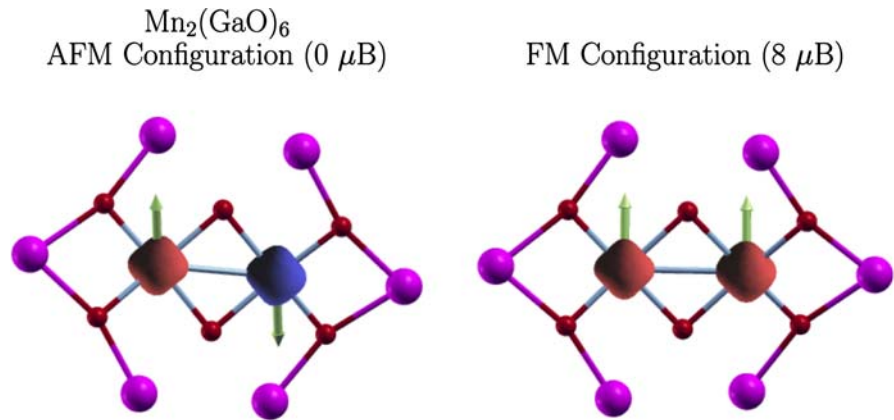
coordination number three. In $Mn_2(GaO)_6$, both Mn are coordinated with four oxygens. Furthermore, addition of GaO to $Mn_2(GaO)_6$ tends to increase the number of Ga–O bonds in the cluster, since the coordination number for Mn atoms remains four. Overall, addition of a Mn atom to $Mn(GaO)_n$ increases slightly (about 2%) the R_{Mn-O} and R_{Ga-O} bond lengths in the ground state configurations.

The overall trend for both Mn- and Mn_2-series shows that the Mn atoms prefer to maximize the Mn–O bonds in the ground state configurations. The preference of $Ga_4(MnO_4)$ is seen in larger clusters with $n > 3$. Addition of second Mn atom to $Mn(GaO)_n$ appears to slightly decrease the relative stability of $Mn_2(GaO)_n$ up to $n = 3$. On the other hand, stability of Mn_2 doped clusters is slightly higher than that of host $(GaO)_n$ cluster with $n > 3$. Successive addition of GaO increases the coordination of Mn atoms resulting into the enhancement of stability of these clusters.

The enhanced stability of the doped clusters is further reinforced by examining the fragmentation energies[2] involving the fragmentation channels via a Mn atom or a GaO molecule. The calculated fragmentation energies (eV) associated with the $Mn(GaO)_n$ ($Mn_2(GaO)_n$) clusters for the loss of a Mn atom are 3.9 (1.34), 4.79 (1.36), 4.75 (2.07), 4.70 (3.07), 5.11 (3.63), 4.06(5.25) and 4.71(3.72) for $n = 1-7$, respectively.

The energies associated for the loss of a GaO are relatively high for both the cluster series considered.

The nature of bonding and magnetic behavior of this series are examined via the charge density isosurfaces of the molecular orbitals and the eigen-value spectrum (not shown) for the ground state and some of the low-lying configurations in this study. The localized charge density distribution is observed around both Mn atoms and oxygens. The nature of bonding remain same as that of Mn doped $(GaO)_n$ clusters. The highest occupied molecular orbital (HOMO) of the ground state configurations consists of Mn_d and O_p orbitals as shown in Fig. 5 for $Mn_2(GaO)_5$.

The calculated magnetic moment of the $Mn_2(GaO)_n$ clusters alternates between 0 and 9 μB (Table 2). Note that the magnetic moments of the $Mn(GaO)_n$ clusters directly depend on the number of Mn–O bonds. Addition of one more Mn atom increases the Mn–O interactions as well as the Mn–Mn interactions in the cluster series. Therefore, the variation in the magnetic moment in $Mn_2(GaO)_n$ is found to be associated with the variation in coordination number of Mn atoms as well as R_{Mn-Mn}. In Mn_2, it has been shown (Kabir et al. 2006) that decrease in $R_{Mn–Mn}$ results into decrease of its magnetic moment, and the stability of the ferromagnetic or antiferromagnetic state depends mainly on the Mn–Mn interactions. From Table 2, as the Mn–Mn distance decreases, quenching of the magnetic moments occurs due to increase in the hybridization between Mn_d and O_p orbitals. On the other hand, two Mn atoms get coupled ferromagnetically in $Mn_2(GaO)_5$ due to increase in $R_{Mn–Mn}$ in its ground state configuration. The ferromagnetic coupling involving nonbonding d orbitals is shown in Fig. 5.

---

[2] The fragmentation energies for $Mn_m(GaO)_n$ cluster are calculated as

$$\Delta^1 E = E[(GaO)_n Mn_m] - (E[(GaO)_n Mn_{m-1}] + E[Mn]),$$
$$\Delta^2 E = E[(GaO)_n Mn_m] - (E[(GaO)_{n-1} Mn_m] + E[GaO]),$$

where E is the total energy of the system.
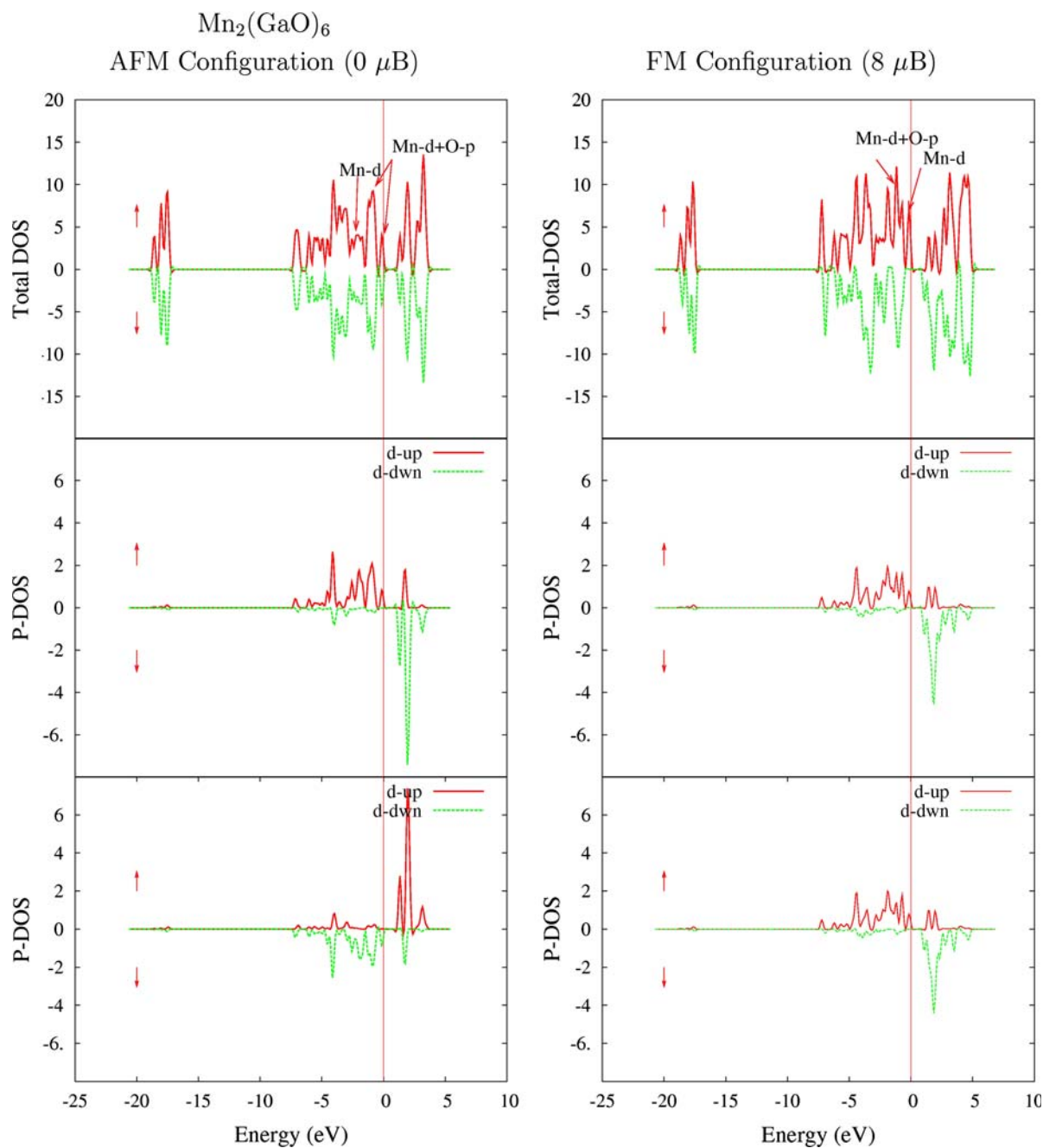
Fig. 7 (Color online) Total Density of States (DOS) and Partial DOS associated with Mn atoms for $Mn_2(GaO)_6$—antiferromagnetic and ferromagnetic configuration. The Fermi level is given by *dotted line* and aligned to zero

For larger clusters, different coordination numbers for Mn atoms result into an inhomogeneous distribution of the Mn_d orbitals which, in turn, increases the magnetic moment to 9 µB.

For $Mn_2(GaO)_6$, antiferromagnetic and ferromagnetic states are nearly degenerate $\Delta E = 0.08$ eV antiferromagnetic state being the ground state. For $Mn_2(GaO)_7$, the AFM state is relatively more stable

showing a small magnetic moment of 1 μB due to an odd number electrons in the cluster.

Figure 6 shows the spin density $[\rho_\uparrow(\mathbf{r}) - \rho_\downarrow(\mathbf{r})]$ for $Mn_2(GaO)_6$, AFM and FM configuration. It is seen that, for AFM configuration, there is equal alignment of spin up and spin down densities on both the Mn atoms quenches completely the cluster magnetic moment. For FM configuration, the positive magnetization density is seen on Mn atoms. The major spin up contribution on Mn atoms originates the large cluster magnetic moment (8 μB).

From the total density of states (DOS) for $Mn(GaO)_n$ and $Mn_2(GaO)_n$ clusters (not shown) it is observed that the successive addition of GaO leads to the broadening of the majority and minority spins. The total and partial DOS further provide an explanation of the magnetic behavior of these clusters. The majority spin Fermi level passes through the hybridized Mn_d–O_p state for small clusters. In the larger clusters, the degree of hybridization increases due to increase in the coordination number for Mn atoms which shifts the Mn_d states below the Fermi level. Figure 7 shows the total-DOS along with the projected-DOS associated with Mn atoms for $Mn_2(GaO)_6$ antiferromagnetic and ferromagnetic configuration. For antiferromagnetic and ferromagnetic configuration the Mn–Mn distance is 2.71 and 2.76 Å, respectively. With the decrease in Mn–Mn distance, increase in the hybridization between Mn_d and O_p orbitals is observed. The hybridized Mn_d–O_p levels are observed near Fermi. The nonbonding Mn_d orbitals shift away from the Fermi which results in quenching of the magnetic moments. In the antiferromagnetic state of $Mn_2(GaO)_6$, the projected DOS show spin up and spin down states below Fermi level to be symmetric. On the other hand, with the increase in Mn–Mn distance, total DOS show the nonbonding Mn_d orbitals near Fermi. The projected DOS of the ferromagnetic $Mn_2(GaO)_6$ show the localized spin-up component resulting into the magnetic moment of 8 μB.

The results find that the degree of coordination of Mn with oxygen plays an important role in determining the magnetic properties of these clusters. As the number of Mn increases, the ferromagnetic coupling stabilizes the cluster when two Mn substitute Ga atoms having different coordination number. Note that the maximum coordination for Mn atom in $Mn(GaO)_n$ and $Mn_2(GaO)_n$ clusters, $(n = 1-7)$ is four. Our results for subnanometer clusters are consistent with the experimental (Huang et al. 2007) results on the bulk Mn doped β-Ga_2O_3.

Conclusions

Stability and magnetic properties of small clusters of $Mn(GaO)_n$ and $Mn_2(GaO)_n$, $(n = 1-7)$ are studied using density functional theory. The overall trend shows that Mn atoms prefer to bind oxygen atoms thereby maximizing their coordination. The magnetic properties appear to be the outcome of a delicate interplay of interactions between Mn–O and Mn–Mn atoms leading to either an antiferromagnetic or a ferromagnetic state in the $Mn_2(GaO)_n$ cluster series.

References

Blanco MA, Sahariah MB, Jiang H, Costales A, Pandey R (2005) Energetics and migration of point defects in Ga₂O₃. Phys Rev B 72:184103-1–184103-16

Blöchl PE (1994) Projector augmented-wave method. Phys Rev B 50:17953–17979

Deshpande M, Kanhere DG, Pandey R (2006) Structural and electronic properties of neutral and ionic Ga_nO_n clusters with $n = 4-7$. J Phys Chem A 110:3814–3819

Dietl T, Ohno H, Matsukura F, Cibert J, Ferrand D (2000) Zener model description of ferromagnetism in Zinc-Blende magnetic semiconductors. Science 287:1019–1020

Gowtham S, Costales A, Pandey R (2004) Theoretical study of neutral and ionic states of small clusters of Ga_mO_n $(m, n = 1-2)$. J Phys Chem B 108:17295–17300

Gowtham S, Deshpande M, Costales A, Pandey R (2005) Structural, energetic, electronic, bonding, and vibrational properties of Ga₃O, Ga₃O₂, Ga₃O₃, Ga₂O₃, and GaO₃ clusters. J Phys Chem B 109:14836–14844

Gutsev GL, Rao BK, Jena P, Wang XB, Wang LS (1999) Origin of the unusual stability of MnO_4^-. Chem Phys Lett 312:598–605

Hayashi H, Huang R, Ikeno H, Oba F, Yoshioka S, Tanaka I, Sonoda S (2006) Room temperature ferromagnetism in Mn-doped γ-Ga₂O₃ with spinel structure. Appl Phys Lett 89:181903-1–181903-3

Huang R, Hayashi H, Oba F, Tanaka I (2007) Microstructure of Mn-doped γ-Ga₂O₃ epitaxial film on sapphire (0001) with room temperature ferromagnetism. J Appl Phys 101:063526-1–063526-6

Kabir M, Mookerjee A, Kanhere DG (2006) Structure, electronic properties, and magnetic transition in manganese clusters. Phys Rev B 73:224439-1–224439-11

Kresse G, Furthmuller J (1996) Efficient iterative schemes for ab initio total-energy calculations using a plane-wave basis set. Phys Rev B 54:11169–11186

Kresse G, Joubert D (1999) From ultrasoft pseudopotentials to the projector augmented-wave method. Phys Rev B 59:1758–1775

Lee SW, Ryu YG, Ahn HY, Park SI, Kim CS (2004) Ferromagnetic effects on transition metal doped Ga_2O_3-based semiconductor. Phys Stat Sol (C) 1:3550–3553

Pei G, Xia C, Dong Y, Wu B, Wang T, Xu J (2008) Studies of magnetic interactions in Mn-doped β-Ga_2O_3 from first-principles calculations. Scripta Materialia 58:943–946

Perdew JP, Burke K, Ernzerhof M (1996) Generalized gradient approximation made simple. Phys Rev Lett 77:3865–3868

Song YP, Wang PW, Xu XY, Wang Z, Li GH, Yu DP (2006) Magnetism and photoluminescence in manganese-gallium oxide nanowires with monoclinic and spinel structures. Physica E 31:67–71

Vienna Ab initio Simulation Package (VASP) (1999) Technische Universität Wien, Vienna